J Biol Inorg Chem (2008) 13:435–447
DOI 10.1007/s00775-007-0332-9

ORIGINAL PAPER

Antioxidant effects of the VO(IV) hesperidin complex and its role in cancer chemoprevention

Susana Beatriz Etcheverry · Evelina Gloria Ferrer · Luciana Naso · Josefina Rivadeneira · Victoria Salinas · Patricia Ana María Williams

Received: 21 September 2007 / Accepted: 5 December 2007 / Published online: 21 December 2007
© SBIC 2007

Abstract Vanadium compounds are known for a variety of pharmacological properties. Many of them display antitumoral and osteogenic effects in several cell lines. Free radicals induce the development of tumoral processes. Natural polyphenols such as flavonoids have antioxidant properties since they scavenge different free radicals. For these reasons it is interesting to investigate the effects of a new complex generated between the vanadyl(IV) cation and the flavonoid hesperidin. The complex has been synthesized and characterized by physicochemical methods. Spectroscopic analysis revealed a 1:1 stoichiometry of ligand:VO and coordination by deprotonated *cis*-hydroxyl groups to the disaccharide moiety of the ligand. The complex improves the superoxide dismutase (SOD)-like activity of the ligand, but the scavenging of other radicals tested does not change upon complexation. When tested on two tumoral cell lines in culture (one of them derived from a rat osteosarcoma UMR106 and the other from human colon adenocarcinoma Caco-2), the complex enhanced the antiproliferative effects of the free ligand, and this effect correlated with the morphological alterations toward apoptosis. Also, on the osteoblastic cell line the complex stimulated cell proliferation and collagen type I production at low concentrations. At higher doses the complex behaved as a cytotoxic compound for the osteoblasts.

Keywords Antioxidants · Antitumoral · Vanadium hesperidin complex · Cellular morphology

Abbreviations

ABTS	2,2′-Azino-bis(3-ethyl-benzothiazoline-6-sulfonic acid diammonium salt)
ALP	Alkaline phosphatase
DMEM	Dulbecco's modified Eagles medium
$DPPH^{\cdot}$	1,1-Diphenyl-2-picrylhydrazyl radical
EDTA	Ethylenediaminetetraacetic acid
NADH	Nicotinamide adenine dinucleotide
NBT	Nitroblue tetrazolium
PMS	Phenazine methosulfate
p-NP	*p*-Nitrophenol
p-NPP	*p*-Nitrophenylphosphate
SOD	Superoxide dismutase
TEAC	Trolox-equivalent antioxidant coefficient
Trolox	6-Hydroxy-2,5,7,8-tetramethylchroman-2-carboxylic acid

Introduction

The damaging intervention of free radicals in normal metabolic processes leading to pathologic changes is a consequence of their interactions with various biological compounds inside and outside cells. There are present numerous natural free radical scavengers and antioxidants that can protect biomolecules against the attack of free radicals and/or suppress the resultant injury. Among these antiradicals, flavonoids are a group of natural occurring

S. B. Etcheverry · E. G. Ferrer · L. Naso · J. Rivadeneira · V. Salinas · P. A. M. Williams (✉)
Centro de Química Inorgánica (CEQUINOR/CONICET,UNLP),
Facultad de Ciencias Exactas,
Universidad Nacional de La Plata,
C. Correo 962, 1900 La Plata, Argentina
e-mail: williams@quimica.unlp.edu.ar

S. B. Etcheverry · J. Rivadeneira
Cátedra de Bioquímica Patológica,
Facultad de Ciencias Exactas,
Universidad Nacional de La Plata,
47 y 115, 1900 La Plata, Argentina

polyphenols predominantly synthesized by higher plants, including moss and ferns [1–4]. Humans consume substantial amounts of flavonoids, since they are present in plant-related foods including fruits, vegetables, oils, nuts, and herbs, and in beverages such as wine, tea, coffee and beer [5, 6]. The antioxidant effects of flavonoids are supposedly due to their free radical scavenging activities [7]. Indeed, flavonoids are able to scavenge superoxide anions, hydroxyl and peroxy radicals, NO radicals, and peroxynitrite. Actually, extensive evidence points to the beneficial clinical and curative effects of flavonoids in the treatment of virus infection, inflammation, diabetes mellitus, headache, etc., in humans [8, 9]. Flavonoids are also effective metal ion chelators [8, 10–12]. As transition metal ions play a vital role in the initiation of free radical processes (via Fenton reactions), metal chelation is widely considered to be another mechanism of antioxidant activity for flavonoids. It has been found that these chelates are much more potent as superoxide radical scavengers than their corresponding uncomplexed flavonoids in a xanthine oxidase/hypoxanthine superoxide-generating system [4, 13].

The flavonoid hesperidin is a flavanone glycoside (glucoside) comprising the flavanone (a class of flavonoids) hesperitin and the disaccharide rutinose. Hesperidin is the predominant flavonoid in lemons and oranges. The peel and membranous parts of these fruits have the highest hesperidin concentrations. Therefore, orange juice containing pulp is richer in this flavonoid than that without pulp. Sweet oranges (*Citrus sinensis*) and tangelos are the richest dietary sources of hesperidin. Hesperidin is classified as a citrus bioflavonoid. The disaccharide of hesperidin, rutinose, comprises the sugars rhamnose (6-deoxy-L-mannose) and glucose. Hesperidin is also known as hesperetin 7-rhamnoglucoside, hesperetin-7-rutinoside and (*S*)-7-[[6-0-(6-deoxy-alpha-L-mannop-yranosyl)-beta-D-glucopyranosyl] oxy]-2,3-dihydro-5-hydroxy-2-(3-hydroxy-4-methoxyphenyl)-4*H*-1-benzopyran-4-one (Fig. 1).

Hesperidin has been reported to have antioxidant, anti-inflammatory, antiallergenic, antihypertensive, antimicrobial, hypolipidemic, anticarcinogenic and vasodilatory properties and to decrease bone density loss [14–16]. Studies with rats treated with orange juice [17] and mandarin juice [18] showed a reduction in colon and lung cancer, as well as the inhibition of atherosclerosis, cholesterol and triglycerides. The antioxidant effect of hesperidin has been previously demonstrated using its capacity to sequester 1,1-diphenyl-2-picrylhydrazyl ($DPPH^{\cdot}$) and eukaryotic cells (of superoxide dismutase-proficient and deficient strains of *Saccharomyces cerevisiae*) treated with hesperidin and the stressing agents hydrogen peroxide or paraquat (methylviologen; 1,1′-dimethyl-4,4′-bipyridinium dichloride) [19].

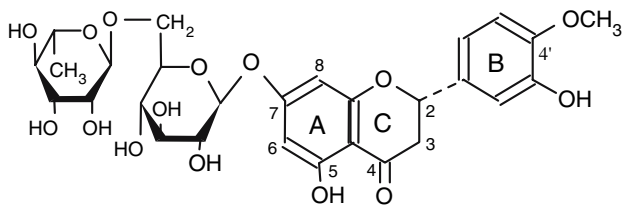

Fig. 1 Structure of hesperidin

Vanadium is an ultratrace element present in higher plants and animals [20–22] which may be beneficial and is possibly essential to humans, but is certainly essential to some living organisms. Its physiological effects in many cases stem from the good complexation behavior of VO^{2+}, and the chemical similarity between phosphate and vanadate. It has been demonstrated that vanadium compounds present interesting biological and pharmacological properties. Vanadium complexes are known to possess potent insulin-mimetic effects, high affinity for several enzymes, and anticancer activity, all of which deserve increasing attention for application to biomedical sciences [23]. Other vanadium complexes have been found to be more effective than the simple vanadium(IV) and (V) salts in experiments performed both in vitro and in vivo [24–26]. Even though a number of simple inorganic vanadium species have beneficial biological properties, the development of new vanadium derivatives with organic ligands to improve their bioavailability and to decrease their toxic side effects is of great interest [27–32].

Taking into account the biological effects of both vanadium and hesperidin alone, a new coordination compound (VOHesp) has been synthesized and physicochemically characterized. The antioxidant effects of hesperidin and the VOHesp complex have been tested using superoxide dismutase (SOD) mimics (enzymatic and nonenzymatic) and their anti-radical activities using $DPPH^{\cdot}$ (1,1-diphenyl-2-picrylhydrazyl radical) and $ABTS^{+}$ [2,2′-azino-bis(3-ethylbenzothiazoline-6-sulfonic acid diammonium salt)]. Since vanadium compounds are distributed between the different tissues and stored mainly in bone once they are absorbed in the organism, it is of special interest to investigate the effect of vanadium derivatives on bone-related cells in culture. For this purpose we have assessed the bioactivity of VOHesp on an osteosarcoma cell line (UMR106). In particular, cell proliferation and osteoblastic differentiation have been determined. Two different markers, collagen type I production and alkaline phosphatase (ALP) specific activity, have been used to evaluate the action of the complex on the differentiation of the osteoblasts. For the sake of comparison, the effect of VOHesp has also been tested on a commercial intestinal bovine ALP. Due to the antitumoral properties of hesperidin it was of great interest to investigate the antiproliferative effect of the free ligand and the

complex on another tumoral cell line derived from a human colon adenocarcinoma (Caco-2). Furthermore, an evaluation of the cytotoxicity of the complex has been accomplished by analyzing the morphological changes caused to both tumoral cell lines by increasing concentrations of the drug.

Materials and methods

Hesperidin (Sigma, St. Louis, MO, USA) and $VOCl_2$ were used as supplied. Crystal violet, *p*-nitrophenylphosphate (*p*-NPP), glycine, $MgCl_2$, nitroblue tetrazolium (NBT), xanthine and xanthine oxidase, DPPH, ABTS and all the other chemicals used were of analytical grade and were obtained from Sigma. Tissue culture materials were purchased from Corning (Princeton, NJ, USA); Dulbecco's modified Eagles medium (DMEM), DMEM low glucose and trypsin–EDTA were from Gibco (Gaithersburg, MD, USA); and fetal bovine serum (FBS) was from Gibco BRL (Life Technologies, Karlsruhe, Germany). IR spectra of powdered samples were measured with a Bruker (Ettlingen, Germany) IFS 66 FTIR spectrophotometer from 4,000 to 400 cm^{-1} in the form of pressed KBr pellets. Electronic absorption spectra were recorded on a Hewlett-Packard (Palo Alto, CA, USA) 8453 diode-array spectrophotometer, using 1-cm quartz cells. Vanadium contents were determined by atomic absorption spectrometry, C and H were determined using a Carlo Erba (Milan, Italy) EA 1108 elemental analyzer and sodium by flame photometry. Thermogravimetric (TG) and differential thermal analysis (DTA) were performed on a Shimadzu (Kyoto, Japan) thermoanalytical system (models TG-50 and DTA-50), working under an oxygen flow (50 mL/min) and at a heating rate of 10 °C/min. Sample quantities ranged between 10 and 20 mg, and Al_2O_3 was used as a DTA standard. A Bruker ESP300 spectrometer operating at the X band was used to record the spectrum of the complex at room temperature in the solid state. A computer simulation of the EPR spectra was performed using the program SimFonia (WINEPR SimFonia v1.25, Bruker Analytische Messtecnik GmbH, 1996).

Preparative

$[VO(Hesp)(OH)_3]Na_4{\cdot}3H_2O$ (VOHesp): an aqueous solution (5 mL) of hesperidin (1 mmol) was prepared adding a concentrated NaOH solution up to pH 12, under a nitrogen atmosphere. A 50% aqueous solution of $VOCl_2$ (0.5 mmol) was added with stirring. The diminution of the pH of the resulting solution produced a green precipitate. This solid dissolves at pH 12, as obtained by the addition of NaOH 1 M. Finally, a green solid complex was obtained using absolute ethanol. This was filtered and washed several times with cold absolute ethanol and air-dried. Anal. calcd. for $C_{28}H_{40}O_{22}VNa_4$: C, 38.6; H, 4.6; V, 5.9; Na, 10.6. Exp.: C, 38.5; H, 4.6; V, 6.0%; Na, 10.4. UV-Vis spectrum: 700 nm. Thermal analysis (TGA) (oxygen atmosphere, velocity, 50 mL/min): in the first step (20–100 °C) three water molecules are lost (6.2%). The dehydrated product $[VO(Hesp)(OH)_3]Na_4$ rendered $NaVO_3$ (characterized by infrared spectroscopy) and Na_2O at 600 °C. The weight of the final residue was 24.7%, in agreement with the theoretical value.

Spectrophotometric titrations

The stoichiometry of the complex was determined by the molar ratio method. An aqueous solution of hesperidin (2×10^{-5} M) was prepared at pH 12 and its electronic spectrum recorded. The absorption spectra of different aqueous solutions of 2×10^{-5} M hesperidin and $VOCl_2$ present in ligand-to-metal ratios from 10 to 0.2 (pH 12) were measured under a nitrogen atmosphere.

SOD assays

The SOD activity was examined indirectly using the NBT assay. The indirect determination of the activities of SOD and the vanadium complex were assayed by their ability to inhibit the reduction of NBT by the superoxide anion generated by the system xanthine–xanthine oxidase at pH 10.2 (0.05 M $NaHCO_3$/NaOH buffer), as reported previously [33, 34]. As the reaction proceeds, the color of formazan develops and a change from yellow to blue is observed, which is associated with an increase in the absorption spectrum at 560 nm. The reaction system contained different concentrations of the flavonoid and its vanadium(IV) complex. The reaction was started by the xanthine–xanthine oxidase system at the concentration needed to yield an absorbance change of between 0.2 and 0.4. Copper(II) chloride aqueous solution, 0.2 mM, was added in order to stop the NBT reduction. Free copper(II) ion is able to interact with the superoxide anion, producing its dismutation. Ethylenediaminetetraacetic acid (EDTA), 0.1 mM, was included due to the formation of a copper chelate (CuEDTA) that has no SOD activity. Each experiment was performed in triplicate, and at least three independent experiments were performed in each case. The amount of complex (or SOD) that gives 50% inhibition (IC_{50}) was obtained by plotting the percentage of inhibition versus the log of the concentration of the tested solution.

The SOD mimetic activity was also determined by a nonenzymatic method, which differs from the enzymatic in the way in which the superoxide radical is generated. In this method, for the system phenazine methosulfate (PMS)/nicotinamide adenine dinucleotide, reduced (NADH) produces the radical anion. The system contains 0.5 mL of sample, 0.5 mL of 1.40 mM NADH, 0.5 mL of 300 μM NBT, in 0.1 M KH_2PO_4/NaOH buffer (pH 7.5). After incubation at 25 °C for 15 min, the reaction was started by adding 0.5 mL of 120 μM PMS [35]. Then the reaction mixture was incubated for 5 min. The results were determined by reading the absorbance at 560 nm against blank samples.

DPPH assays

The antiradical activities of hesperidin and VOHesp were measured in triplicate using a modified Yamaguchi et al. method [36]. A methanolic solution of DPPH (4 mL, 40 ppm) was added to 1 mL of the antioxidant solutions in 0.1 M Tris–HCl buffer (pH 7.1) at 25 °C, giving final concentrations of 10, 25, 50, 100 μM. The absorbance at 517 nm was measured after 60 min of the reaction in the dark and compared with the control prepared in a similar way without the addition of the antioxidants (this value was assigned arbitrarily to 100%). A 100 μM solution of ascorbic acid (a strong antioxidant agent) was also tested as a control for the reaction. In this case, the violet color of $DPPH^{\cdot}$ disappeared immediately.

ABTS decoloration assay

The total antioxidant activity was measured using the Trolox (6-hydroxy-2,5,7,8-tetramethylchroman-2-carboxylic acid)-equivalent antioxidant coefficient (TEAC). The $ABTS^{\cdot+}$ (2,2′-azino-bis(3-ethyl-benzothiazoline-6-sulfonic acid) diammonium salt) radical cation was generated by incubating ABTS with potassium persulfate. Chemical compounds that inhibit the potassium persulfate activity may reduce the production of $ABTS^{\cdot+}$. This reduction results in a decrease in the total $ABTS^{\cdot+}$ concentration in the system and contributes to the total $ABTS^{\cdot+}$ scavenging capacity. Briefly, an aqueous solution of ABTS (2.5 mM) and potassium persulfate (0.4 mM) was incubated in the dark for 24 h. The solution was then diluted ten times in 0.1 M KH_2PO_4/NaOH buffer (pH 7.4). Ten microliters of hesperidin, the complex or the Trolox standard in phosphate buffer were added to 990 μL of this mixture (final concentrations 0–100 μM). The reduction of the $ABTS^{\cdot+}$ radical cation was monitored spectrophotometrically 6 min after initial mixing at 25 °C. The percentage decrease in the absorbance at 734 nm was calculated considering that the basal condition (without antioxidant additions) was taken to be 100% and plotted as a function of the concentration of the samples, giving the total antioxidant activity (TAA). The TEAC was calculated from the slope of the plot of the percentage inhibition of absorbance versus concentration of the antioxidant divided by the slope of the plot of Trolox [37, 38].

Alkaline phosphatase assays

The effect of hesperidin and HespVO on bovine intestinal ALP activity was determined spectrophotometrically, and compared with data on the vanadyl(IV) cation, which is a well-known control for the inhibitory effect of vanadium on ALP specific activity. The solutions of the free ligand and the complex were prepared by dissolving each solid in the buffer solution. The reaction was started upon the addition of the substrate (*p*-NPP), and the generation of *p*-nitrophenol (*p*-NP) was monitored via the absorbance changes at 405 nm. Briefly, the experimental conditions for ALP specific activity measurement were as follows: 1 μg/mL of bovine intestinal ALP and 5 mM of *p*-NPP were dissolved in the incubation buffer (0.2 M glycine/NaOH + 0.55 mM $MgCl_2$, pH 10.5) and left for 10 min. The effects of the compounds were determined by adding different concentrations (10–100 μM) of each one to the pre-incubated mixture. The effect of each concentration was tested at least in triplicate in three different experiments. Basal conditions, in the absence of any compound, were determined as the absorbance of *p*-NPP hydrolysis at 37 °C and pH 10.5. The enzymatic reaction rates inhibited by hesperidin and its vanadium complex were determined just as for the basal conditions but in the presence of the different concentrations of each of the investigated systems. Data were expressed as mean ± SEM. Statistical differences were analyzed by Student's *t*-test.

Cell culture

Rat osteosarcoma UMR106 and human colon adenocarcinoma cell line Caco-2 were grown in DMEM supplemented with 10% (v/v) FBS and antibiotics (100 U/mL penicillin and 100 mg/mL streptomycin) in a humidified atmosphere of 95% air/5% CO_2. When cells reached ca. 90% confluence they were subcultured using 0.1% trypsin-1 mM EDTA in Ca^{2+}–Mg^{2+}-free phosphate-buffered saline (PBS). For experiments, about 6.0×10^4 cells/well (UMR 106) and 1.5×10^5 cells/well for

Caco-2 were plated into 24 wells/plate. After the culture reached 90% confluence, the cells were washed twice with DMEM.

Cell proliferation assay

A mitogenic bioassay was carried out as described by Okajima et al. [39] with some modifications. Briefly, cells in 24 wells/plate were washed with PBS and fixed with 5% glutaraldehyde/PBS at room temperature for 10 min. Cells were then stained with 0.5% crystal violet/25% methanol for 10 min. After that, the dye solution was discarded and the plate was washed with water and dried. The dye in the cells was extracted using 0.5 mL/well 0.1 M glycine/HCl buffer, pH 3.0/30% methanol, and transferred to test tubes. Absorbance was read at 540 nm after a convenient sample dilution. The correlation between cell number/well and the absorbance at 540 nm of diluted extraction sample after crystal violet staining was established previously [40]. Data are expressed as the mean ± SEM. Statistical differences were analyzed using Student's *t*-test. *t*-tests were done to compare treated cultures with the untreated cultures. Freshly prepared solutions of hesperidin, VO(IV), and VOHesp (serum-free DMEM) were added to the culture dishes at the following concentrations: 0, 10, 25, 50 and 100 μM. Cells were incubated overnight with the compounds at different doses in serum-free DMEM.

Osteoblastic differentiation assays

Alkaline phosphatase specific activity

Alkaline phosphatase specific activity has been used as a marker of osteoblast phenotype [41–43]. Cells were grown in 24-well plates until 70–80% confluence, and the monolayers were washed twice with serum-free DMEM. Then the cells were incubated overnight with serum-free DMEM and different doses of VOHesp (10–100 μM) were added. The cell layer was then washed with PBS and solubilized in 0.5 mL 0.1% Triton X-100. Aliquots of the total cell extract (10–20%) were used for protein determination by the Bradford technique [44]. Measurement of ALP activity was carried out by spectrophotometric determination of initial rates of hydrolysis of *p*-NPP to *p*-NP at 37 °C for 10 min. The reaction mixture consisted of 10 μL of cell extract in 800 μL of glycine buffer (0.2 M glycine/NaOH + 0.55 mM $MgCl_2$, pH 10.5). The reaction was initiated by the addition of 100 μL of substrate solution to 5 mM *p*-NPP in glycine buffer. The production of *p*-NP was determined by the absorbance at 405 nm. Under these experimental conditions, product formation was linear for 15 min.

Collagen production

The synthesis of type I collagen is also a marker of osteoblastic phenotype. The effects of VOHesp and hesperidin on this parameter were analyzed by a histochemical method adapted to determine the collagen production by the osteoblasts in the culture [45]. UMR106 cells were cultivated on multi-well plates. When the cells reached 90% confluence, the layers were washed three times with PBS and fixed for 1 h with 1 mL of fixation solution (15 mL of picric acid solution/5 mL of formaldehyde 35% and 1 mL of glacial acetic acid). After that, the monolayers were washed for 15 min with distilled water with mild agitation and then colored with 1 mL of dye solution (Sirius Red 100 mg in 100 mL of a saturated solution of picric acid) for 1 h with mild agitation. They were then washed with HCl 0.01 N to remove the excess of Sirius Red. The dye fixed to the collagen was extracted with 1 mL of NaOH 0.1 N with mild agitation for 30 min. The absorbance of the samples was then recorded at 550 nm. The content of collagen produced by the cells was obtained by the calibration curve obtained under the same conditions as those reported previously [45].

Cell morphology

The cell lines were grown in six wells/plate. The cells were incubated overnight with fresh serum-free DMEM plus 0 (basal), 10, 25, 50 and 100 μM solutions of the complex. The monolayers were subsequently washed twice with PBS, fixed with methanol, and stained with 1:10 dilution of Giemsa for 10 min [46]. Next, they were washed with water and the morphological changes were examined by light microscopy.

Results and discussion

UV-Vis spectra and spectrophotometric titrations

The electronic spectrum of hesperidin was recorded in water (pH 12, using NaOH) under a nitrogen atmosphere. Three peaks were observed in the ligand spectra at 242, 288 and 358 nm [47, 48]. The latter band is related to ring B (cinnamoyl system), and the other bands to ring A (benzoyl system). After the interaction with vanadyl(IV) cation, the bands at higher energy undergo increases in

their intensities and a small blue shift is observed for these two bands (see Fig. 2).

The band at 358 nm remains unchanged, indicating that there is no interaction of the cinnamoyl moiety with the metal center [49]. Spectrophotometric titrations were performed in order to determine the stoichiometry of the VOHesp system, by following the increase of the 242 or the 288 nm bands upon the addition of different quantities of VO(IV). In both cases, in the molar ratio plot [50] the inflection at [L]/[M] 1 is indicative of the formation of a Hesp/VO 1/1 complex (Fig. 2, inset).

The electronic spectrum in the visible region was measured with fresh 5×10^{-4} M aqueous solutions of the complex (pH 12), under a nitrogen atmosphere. A shoulder of high intensity masked the UV part of the spectrum up to 500 nm. A band at 702 nm can be observed, together with an incipient shoulder at 520 nm. Sugar vanadyl(IV) complexes coordinated through deprotonated *cis*-hydroxyl groups show a three-band pattern at ca. 420, 500 and 700 nm [51–53]. It can therefore be concluded that the interaction of the metal center with the ligand occurs through *cis*-OH deprotonated groups of the disaccharide part of hesperidin, rutinose, instead of the typical interaction though the 3-OH group of the cinnamoyl of the flavanone hesperitin. In the present case different interaction behavior of the metal with the flavonoid is observed because of the deprotonation of the sugar hydroxyl groups at the pH value used in the synthesis of the complex. These results are also supported by infrared analysis (see below).

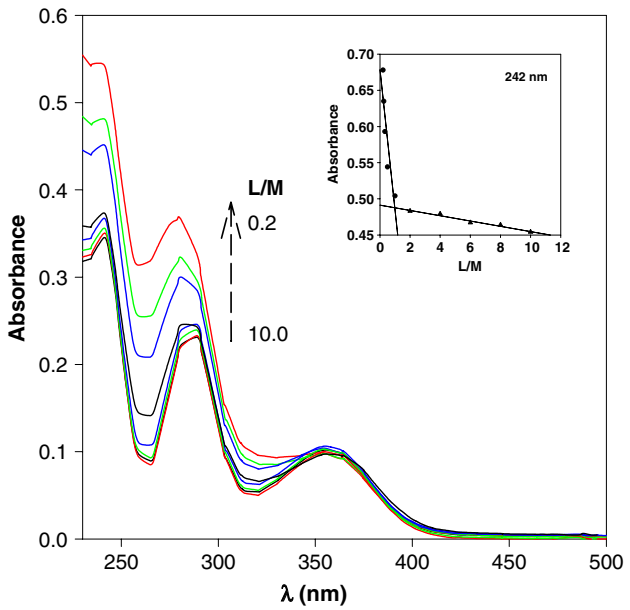

Fig. 2 UV-Vis spectra of hesperidin (2×10^{-5} M) alone and with $VOCl_2$ in ligand-to-metal ratios (L/M) from 10.0 to 0.2 (pH 12), nitrogen atmosphere. The *arrow* indicates increasing metal additions. *Inset* shows spectrophotometric determination of the stoichiometry of the VOHesp complex at 242 nm by the molar ratio method

Infrared spectra

The flavonoid hesperidin is composed of hesperitin and rutinose moieties. For the analysis of the sugar's vibrational modes, the spectrum is divided into the following regions: 1,500–1,150 cm^{-1} for HCH, CH_2OH vibrations; 1,150–950 cm^{-1} for CO stretch; 950–700 cm^{-1} for lateral group bending (COH, CCH, OCH) or the anomeric region [54]. Tentative assignments are shown in Table 1.

The main changes in band intensity and displacement occur in the peaks which involve OH stretches and deformations. These modifications may be due to the deprotonation and/or coordination of the OH sugar groups because of the strong alkaline media used in the preparation of the complex. Because of the presence of the stretching band at 878 cm^{-1} it can be assumed that the glucose residue is bonded to hesperitin in the β-anomer form and that the 818 cm^{-1} band is indicative of the α-anomeric form of the deoximannose residue. The V=O stretch is located at 931 cm^{-1}. The position of this band is indicative of chelate formation around the vanadyl cation, with deprotonated pairs of OH groups in the *cis* position, which is also observed for complexes of VO(IV) with

Table 1 Tentative assignments for the FTIR spectra of hesperidin and VOHesp (band positions in cm^{-1})

Hesperidin	VOHesp	Assignments
1,647 vs	1,644 sh	ν (C=O)
1,609 s	1,612 vs	ν (C=C), ring
	1,582 sh	
1,516 s	1,539 m/1,515 sh	
1,447 m	1,432 m	δ (CH_2)
1,361 m	1,382 w/1370 sh	δ (COH)
1,285 s	1,273 m	δ (COH), ν (C–O–C)
1,196 s	1,207 m/1,176 m	δ (CH_2)
1,129 s	1,132 m	
1,090 sh	1,095 sh	ν $(C–O)_{endo}$
1,072 vs	1,072 vs	ν $(C–O)_{exo}$
1,030 sh	1,030 sh	
975 m	971 m	
	931 sh	ν (V=O)
878 sh	878 vw	δ (C1H), β glucose
818 w	828 sh/814 w	δ (C1H), α deoximannose
743 w	767 sh/732 sh	
671 w	679 w	

s Strong; *vs* very strong; *w* weak; *m* medium; *sh* shoulder; *vw* very weak

different carbohydrates [51–53, 55]. The coodination of the metal to the C(4)=O residue is discarded because this stretching mode remains unaltered (only its intensity is diminished). A new shoulder at 1,582 cm^{-1} can be assigned to a possible deprotonation of the OH group bonded to C(5) of hesperitin which gives rise to electronic delocalization between both groups, with the consequent coupling of the vibrations of these two bonds.

EPR spectroscopy

The monomeric nature of the complex has been determined by EPR spectroscopy at room temperature (see Fig. 3). The EPR spectrum gives an eight-line pattern ($I = 7/2$), confirming the d^1 V(IV) oxidation state. The spin Hamiltonian parameters $g_{\|} = 1.940$, $A_{\|} = 167.10^{-4}$ cm^{-1} agree with those for previously reported vanadyl–saccharide–hydroxyl complexes [56]. Also, the configuration of the complex was assumed to be an axially compressed $d^1{}_{xy}$ pattern: $g_{\|} < g_{\perp}$ ($g_{\perp} = 1.974$) and $A_{\|} > A_{\perp}$ ($A_{\perp} = 55 \times 10^{-4}$ cm^{-1}). In such cases the hyperfine splitting parameters are indicative of the presence of the VO(IV) unit in $VO(O)_4$ environments, with values of $A_{\|}$ and $g_{\|}$ in the range of 149–186 $\times 10^{-4}$ and 1.93–1.96 $\times 10^{-4}$ cm^{-1}, respectively. In the present case the binding mode of this complex could be expected to involve an equatorial coordination sphere with two deprotonated *cis*-OH groups from the sugar moiety and two OH^- anions bound to the vanadyl(IV) center.

Superoxide dismutase activity

The superoxide radical anion has been demonstrated to be a mediator of ischemia, injury, inflammation and vascular diseases. SOD catalyzes the dismutation of superoxide radical anions to the nonradical products oxygen and hydrogen peroxide and protects living cells against the toxicity of hyperoxia. The application of SOD as a pharmaceutical has attracted considerable attention. However, the molecular weights of SODs are too high to cross cell membranes and they can only provide extracellular protection. In order to circumvent this difficulty, a stable nontoxic, low-molecular-weight metal complex that catalyzes the dismutation of superoxide anion might be a suitable alternative to SOD in clinical applications, possessing the advantages of low cost, cell permeability and nonimmunogenicity [57, 58].

Kostyuk et al. [7] reported an IC_{50} value (to reduce 50% of NBT) of 0.15 nM for SOD. IC_{50} values of ca. 1–10 μM have been found for different flavonoids. This effect was enhanced tenfold when metal flavonoid complexes were measured [7]. In the enzymatic method used herein (superoxide is generated by the xanthine–xanthine oxidase reaction), different IC_{50} values were obtained for SOD (0.085 μM), hesperidin (0.43 mM), and VOHesp (94 μM). Nevertheless, the antioxidant power of the flavonoid and the enhancement of this effect by complexation with vanadyl(IV) cation has been demonstrated (see Fig. 4).

Potent SOD mimic compounds display IC_{50} values in the range of 20 μM according to Roberts and Robinson

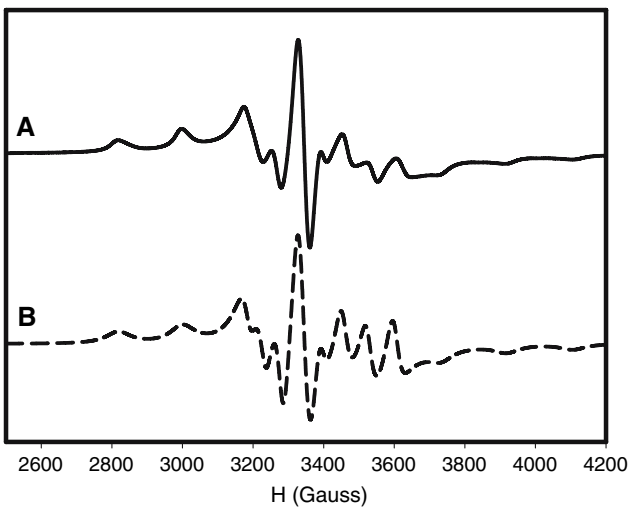

Fig. 3 Experimental (*A*) and calculated (*B*) room-temperature powder EPR spectra of the complex $[VO(Hesp)(OH)_3]Na_4{\cdot}3H_2O$ measured at the X band (9.406 GHz)

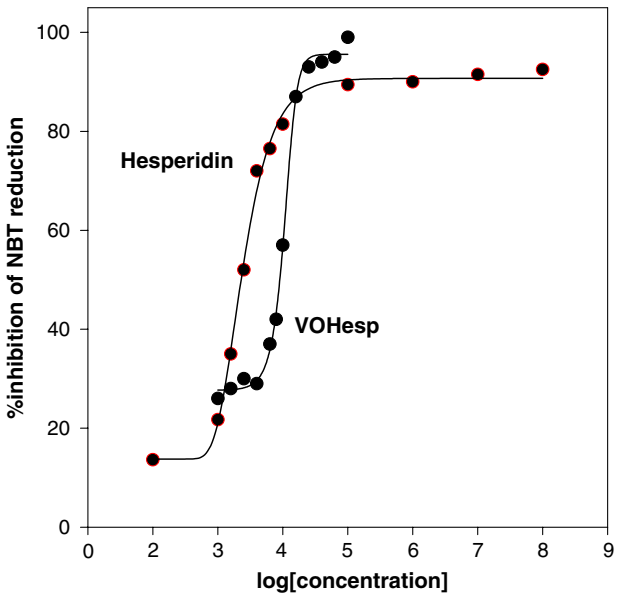

Fig. 4 Effect of hesperidin and $[VO(Hesp)(OH)_3]Na_4{\cdot}3H_2O$ on the reduction of NBT (nitro blue tetrazolium) by enzymatically generated superoxide (xanthine/xanthine oxidase system)

[32]. The present complex is not considered a very potent enzyme analog [59]. Enzymatic assays did not provide conclusive evidence when the tested compounds affected superoxide generation by directly interacting with xanthine oxidase. In such cases, the IC_{50} values for inhibition of NBT reduction and uric acid production were quite close. These issuees can be solved using nonenzymatic assay systems. After generating the superoxide radical by the PMS/NADH system, the VOHesp complex exhibited a potent SOD-like activity of 6 μM (Fig. 5) (IC_{50} values measured for SOD, VO(IV) and for hesperidin were 0.21, 15 μM and 2.23 mM, respectively).

Through two different experimental techniques it was demonstrated that hesperidin is able to scavenge superoxide radicals at high concentrations but that its complexation with vanadyl(IV) cation improves this ability, as has been previously proved for other flavonoid metal complexes [7]. The SOD mimetic behavior of hesperidin is similar to those of naringenin, 4′-hydroxyflavanone, 3-hydroxyflavone compounds, and many flavonoid derivatives with IC_{50} values that are higher than 30 μM [13].

Scavenging of the DPPH· radical

A simple chemical assay that is broadly applicable for determining the hierarchy of antioxidant activities of polyphenols measures their ability to sequester 1,1-diphenyl-2-picrylhydazyl (DPPH·). When scavenging of the DPPH· radical was tested for hesperidin, the strongest activity was observed at higher concentrations. Significantly higher antiradical power was displayed by the complex at 50 and 100 μM compared to hesperidin. The antioxidant activity of hesperidin was previously established using the DPPH· method by Wilmsen et al. [19]. In this work we obtained a lower value for the antioxidant capacity (in five different determinations, each one performed in triplicate), but the experimental conditions used here were a little different (25 °C, absence of DMSO and pH 7.1). Anyway, the aim of this work is to determine the improvement in the activity of the flavonoid upon complexation with a metal. In this context, we have found that the vanadyl(IV) cation does not alter the antioxidant capacity of hesperidin, or at least its activity is only poorly enhanced by complexation (Fig. 6).

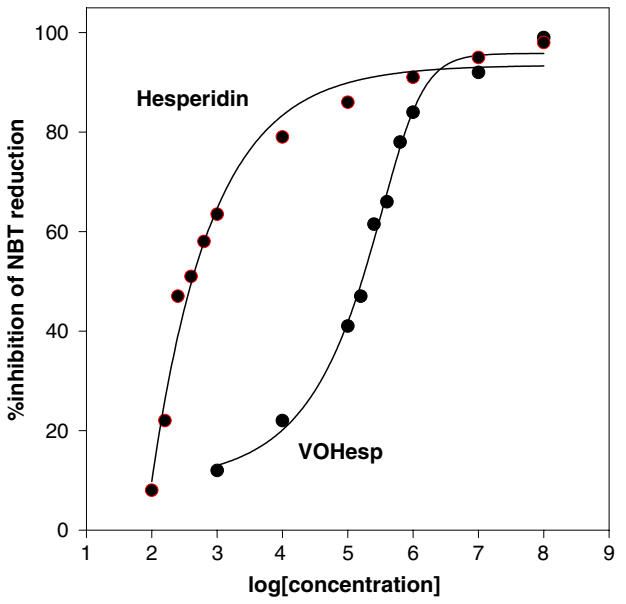

Fig. 5 Effect of hesperidin and $[VO(Hesp)(OH)_3]Na_4{\cdot}3H_2O$ on the reduction of NBT (nitro blue tetrazolium) by nonenzymatically generated superoxide (phenazine methosulfate/NADH system)

Total antioxidant activity and Trolox-equivalent antioxidant coefficient

The total antioxidant activities of hesperidin, VOHesp and Trolox are displayed in Fig. 7, which shows the dependence of the inhibition on the concentrations of the compounds. The percentage inhibition of the $ABTS^{\cdot+}$ radical cation is concentration-dependent. The TEAC was calculated from the slopes of these plots. The Trolox-equivalent antioxidant capacities of hesperidin and VOHesp were 0.67 and 0.61, respectively. The TEAC value for hesperidin is lower than those for flavonoids such as quercetin due to structural differences. The former compound has a 4′-methoxy group in

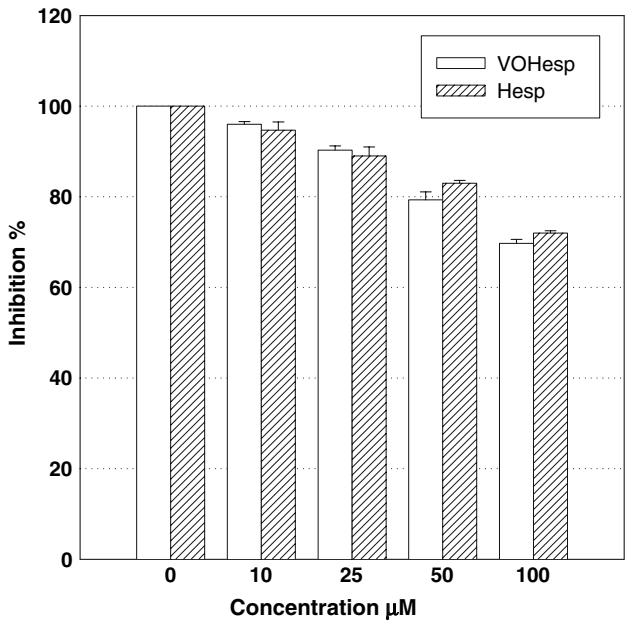

Fig. 6 Effects of hesperidin and $[VO(Hesp)(OH)_3]Na_4{\cdot}3H_2O$, VOHesp, on the reduction in the concentration of DPPH·. Values are expressed as the mean ± standard error of the mean (SEM) of at least three independent experiments

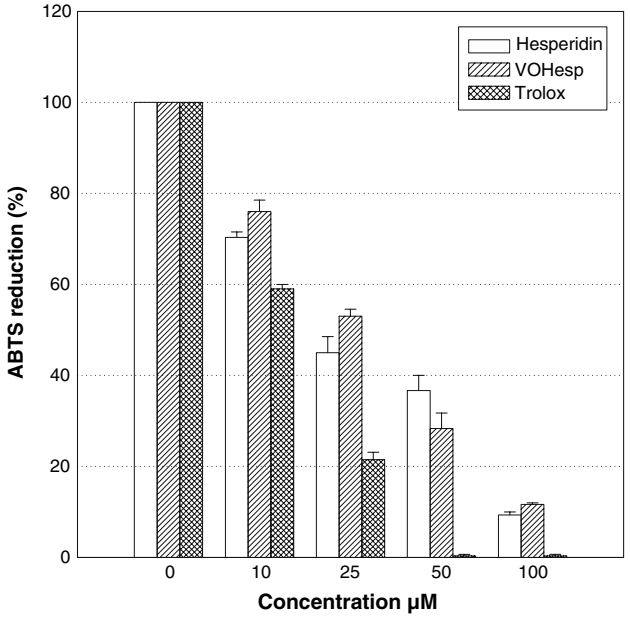

Fig. 7 Total antioxidant activity (TAA), measured as the reduction in the concentration of $ABTS^{\cdot+}$ caused by the addition of hesperidin, $[VO(Hesp)(OH)_3]Na_4{\cdot}3H_2O$, VOHesp, and Trolox. Values are expressed as the mean ± standard error of the mean (SEM) of at least three independent experiments

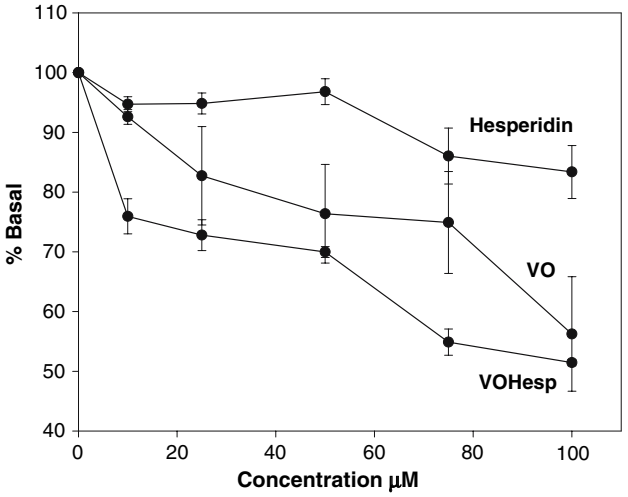

Fig. 8 Effects of hesperidin, $[VO(Hesp)(OH)_3]Na_4{\cdot}3H_2O$ and VO(IV) on the activity of mucose bovine intestinal alkaline phosphatase. The initial rate was determined by incubating the enzyme at 37 °C for 10 min in the absence and presence of various concentrations of the inhibitors. Values are expressed as the mean ± standard error of the mean (SEM) ($n = 9$)

the B ring and a glycosylated seventh position in the A ring, while the highest activity for quercetin relates to the activity of the *o*-dihydroxy structure in the B ring and the unsaturated C ring, with its 3-hydroxyl group, linking with the 5,7-dihydroxy structure in the A ring. On the other hand, kaempferol (in which the catechol structure has been substituted in the flavon-3-ol B ring for a phenolic ring with a single 4′-hydroxyl group) shows a somewhat higher antioxidant activity than that of hesperidin, and this may be due to the substitution in the seventh position of the A ring of the latter compound, which further decreases the antioxidant activity.

Altogether, these results again point to the similar antioxidant behaviors of the flavonoid and its vanadyl(IV) complex. The antioxidant power of hesperidin is high and comparable to those of other flavonoids with 5-OH and 4-keto groups that provide a catechol-like structure in rings A and C [60]. The complexation with the vanadyl(IV) cation does not improve the antioxidant capacity, possibly because the coordination of the metal occurs in the saccharide moiety and so it does not alter the abovementioned structure.

Alkaline phosphatase inhibition

Alkaline phosphatase is an enzyme that is widely distributed in living organisms. It hydrolyzes phosphate esters and it forms an activated complex with the substrate that has a trigonal bipiramidal structure. The inhibitory effect of vanadium compounds on the activities of enzymes that catalyze phosphate group transfer may be due to the formation of a similar transition state conformation. However, bonds with vanadium compounds are stronger than those with phosphate groups. This greater stability of the transition state complex explains the inhibition of the reaction by vanadium derivatives.

The inhibitory effects of the metal, the ligand and the complex on ALP activity are shown in Fig. 8. Free hesperidin does not produce inhibition at concentrations of up to 50 μM. A slight inhibitory effect has been observed at higher concentrations (15% at 100 μM). On the other hand, the VOHesp complex produced inhibition in a dose–response manner, which is higher than that of the ligand and free VO(IV). 50% inhibition was detected at a concentration of 100 μM.

Effect of VOHesp on cell growth

The action of hesperidin on cellular proliferation was measured for both cell lines in the concentration range of 0–100 μM. The flavonoid caused a slight inhibition of up to ca. 10% in cell proliferation in the tested concentration range. The effects of the VOHesp complex on the UMR106 rat osteosarcoma-derived cells and Caco-2 human colon adenocarcinoma cell lines are displayed in Figs. 9 and 10. The complex exhibited cytotoxicity on both cell lines in a dose–response manner.

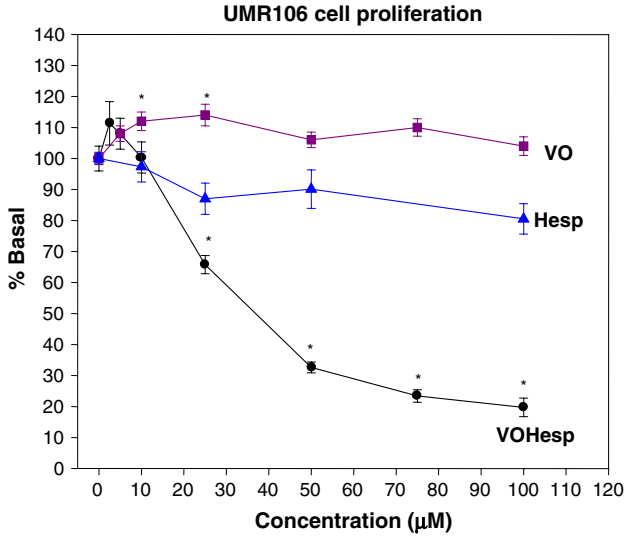

Fig. 9 Effects of hesperidin, $[VO(Hesp)(OH)_3]Na_4{\cdot}3H_2O$ and VO(IV) on UMR106 osteoblast-like cell proliferation. Cells were incubated in serum-free DMEM alone (basal) or with different concentrations of the compounds at 37 °C for 24 h. Results are expressed as % basal and represent the mean ± SEM, $n = 9$. $^*P < 0.001$

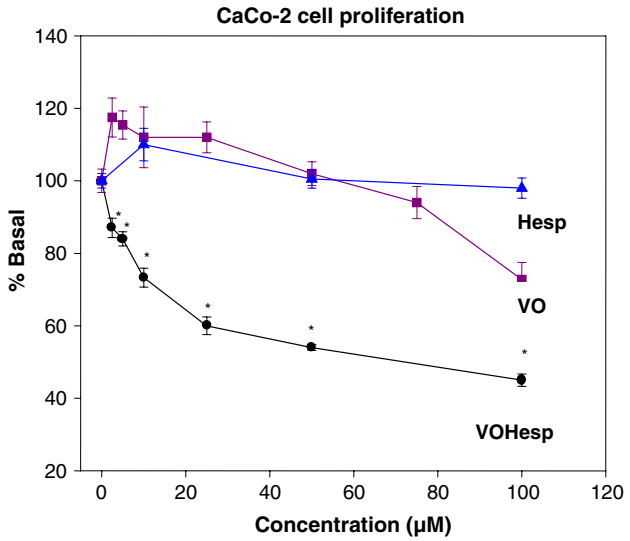

Fig. 10 Effects of hesperidin, $[VO(Hesp)(OH)_3]Na_4{\cdot}3H_2O$ and VO(IV) on human colon adenocarcinoma Caco-2 cell proliferation. Cells were incubated in serum-free DMEM alone (basal) or with different concentrations of the compounds at 37 °C for 24 h. Results are expressed as % basal and represent the mean ± SEM, $n = 9$. $^*P < 0.001$

In UMR106 cells (Fig. 9), the complex slightly stimulated cell growth over a narrow range of concentrations (2.5–10 μM, $P < 0.001$) and inhibited cell proliferation at doses of 25–100 μM (80% at 100 μM).

In Caco-2 cells, the complex was highly cytotoxic from 2.5 to 10 μM, decreasing the cell number across the whole range of concentrations in a dose–response manner. Nevertheless, at 50 and 100 μM, VOHesp caused a stronger inhibition in UMR106 than in the adenocarcinoma cell line (the survival cells were 55% of the basal at 100 μM) (Fig. 9). The antiproliferative effect of the vanadium(IV) complex was also compared with the effect of the vanadium(IV) cation on both cell lines. The addition of VO(IV) to the culture media significantly stimulated UMR106 cell proliferation ($P < 0.01$). In Caco-2, the effect of VO was rather deleterious only at 100 μM.

Osteoblast differentiation assays

To evaluate the effects of the complex on cell differentiation, its action on ALP specific activity and collagen type I synthesis was investigated in UMR106 cells. The action of VOHesp on the osteoblastic ALP specific activity can be observed in Fig. 11. The complex produced standard inhibitory agent behavior, similar to free vanadyl(IV) cation [61]. On the other hand, the reduction in the enzyme activity caused by the presence of the free ligand, hesperidin, was very small. This pattern was also observed for the activity of bovine mucose intestinal ALP (Fig. 8).

Collagen type I is one of the most abundant and important components of the extracellular matrix. This protein is produced by living cells like osteoblasts in culture and is considered to be another marker of cell differentiation. Figure 12 shows the effect of the complex on this parameter. The collagen production was measured in a confluent monolayer in the range 2.5–10.0 μM, where

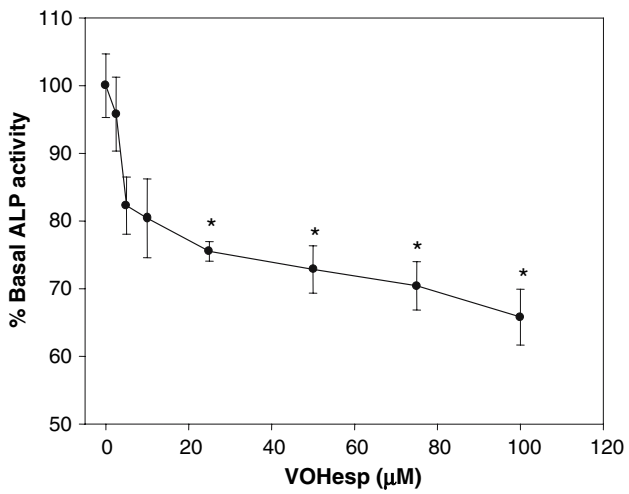

Fig. 11 Effect of $[VO(Hesp)(OH)_3]Na_4{\cdot}3H_2O$ on ALP specific activity. UMR106 cells were incubated either in serum-free DMEM alone (basal) or with different concentrations of the compound at 37 °C for 24 h. Basal activity was nM pNP/min × mg protein. Results are expressed as % basal and represent the mean ± SEM, $n = 9$. $^*P < 0.002$

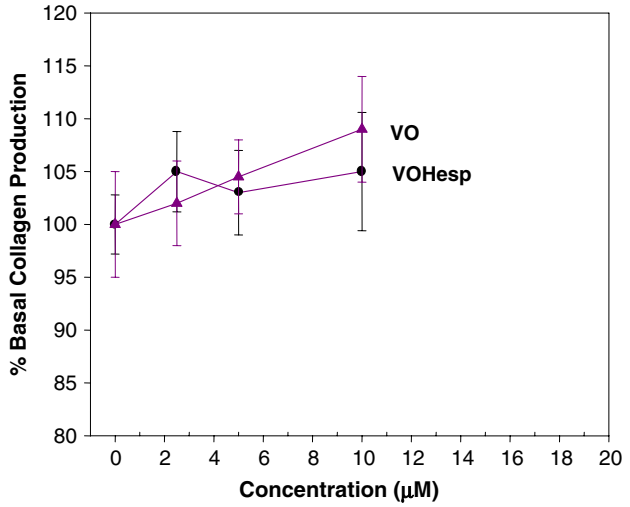

Fig. 12 Synthesis of type I collagen: effects of $[VO(Hesp)(OH)_3]$-$Na_4 \cdot 3H_2O$ and VO(IV) on UMR106 cells. The cells were cultivated on multi-well plates up to 100% confluence in the absence (basal) or in the presence of the compounds. After fixation, the monolayers were colored with Sirius Red. The absorbance of the samples was recorded at 550 nm. Results are expressed as % basal and represent the mean ± SEM, $n = 9$

no toxic effects of the complex were observed. VOHesp and VO(IV) slightly promoted the synthesis of collagen up to 10.0 μM. Hesperidin did not exert any effect on this parameter.

These observations showed that the vanadium hesperidin complex behaved as an inhibitory agent towards osteoblastic proliferation and also towards their differentiation (at concentrations higher than 25 μM). At lower concentrations, VOHesp slightly induced osteoblastic cell proliferation and collagen type I production.

Cell morphology

The ability of VOHesp, VO(IV) ions and hesperidin to induce morphological changes was investigated in the two cultured cell lines. After overnight incubation in a serum-free medium with or without the addition of the compounds, the cells were fixed, stained and observed by light microscopy.

For UMR106 cells, the control (medium alone) showed a polygonal morphology with irregular nuclei, many of which had a kidney-like shape that exhibited large numbers of nucleoles. Cells displayed numerous intercellular connections and some mitotic figures (Fig. 13). When incubated with vanadium, a few cells exhibited a trapezoidal form and a few had very long intercellular connections. The nuclei were condensed with vacuoles in their interior. It was not possible to distinguish the nucleoles (data not shown). Even though the morphological transformations were determined for all of the tested concentrations, only the results at 50 and 100 μM were shown, since at these concentrations the alterations in morphology are the most remarkable. The complex induced a significant decrease in the number of surviving cells as well as morphological alterations (Fig. 13b, c). The nuclei displayed dense chromatin granules and many membrane blebs, indicating an active apoptosis process (Fig. 13b). At 100 μM a marked reduction in the number of cells and a tendency for them to group was observed. The cytoplasm showed strong condensation with the loss of processes (Fig. 13c).

The characteristics of the Caco-2 cells can be observed in Fig. 14. The cells displayed a polyhedral form with big nuclei and numerous nucleoles. Like UMR106, several intercellular connections and mitotic figures were observed (Fig. 14a) [62]. Upon incubation with vanadium, the cytoplasmatic borders became weakly visible. Numerous irregular vacuoles were observed in the cytoplasm. The nuclei are condensed without visible nucleoles (data not shown). After the addition of VOHesp to the cell culture, a dose–response effect on the number of surviving cells was observed when the concentration increased from basal to 100 μM. These results parallel those obtained from the proliferative studies. At 50 and 100 μM the nuclei were more condensed and irregular (Fig. 14b, c). There were many irregular vacuoles in the cytoplasmatic region. Also, under the action of the complex, this cell line showed a great tendency to form groups or clusters of cells. When the cells of the two cell lines were incubated with hesperidin they grew well and without morphological alterations in the two cell lines.

Conclusions

Our physicochemical characterization of the new vanadyl hesperidin complex (VOHesp) allowed us to conclude that the metal interacts with the ligand through *cis*-deprotonated OH groups of the rutinose disaccharide. The improvement in the antioxidant activity of hesperidin upon complexation with VO(IV) was demonstrated by the fact that it became a better SOD mimic. Nevertheless, considering the capacities of hesperidin and the vanadyl(IV) complex to sequester the radicals $DPPH^{\cdot}$ and $ABTS^{\cdot+}$, it can be seen that both compounds have similar sequestering capacities and flavonoid antioxidant capacities. In this context, complexation did not improve the antioxidant power of hesperidin. This fact may be due to the coordination of the vanadyl(IV) cation through the rutinose moiety of the ligand, leaving the flavonol part unmodified. These results indicate that both the free ligand and the complex are promising agents for

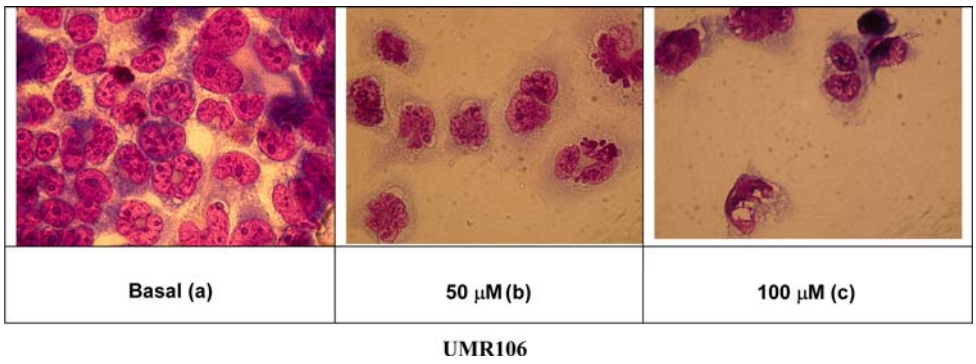

Fig. 13 Effect on cell morphology for the treatment of the osteosarcoma UMR106 cells without drug addition (control) (**a**), with 50 μM VOHesp (**b**) and with 100 μM VOHesp (**c**) (obj. ×100)

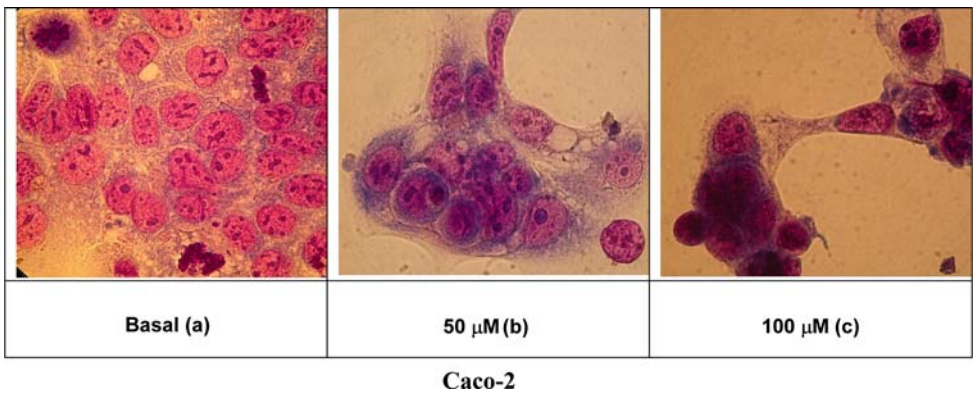

Fig. 14 Effect on cell morphology for the treatment of the human colon adenocarcinoma Caco-2 cells without drug addition (control) (**a**), with 50 μM VOHesp (**b**) and with 100 μM VOHesp (**c**). (obj. ×100)

preventing pathologies in which free radicals are implicated, such as degenerative diseases, cancer, etc.

In the biological studies, VOHesp behaved as a more deleterious compound for UMR106 osteoblast-like cells than for the Caco-2 human colon adenocarcinoma line in the middle and upper ranges of the tested doses. However, at low concentrations it slightly stimulated osteoblast proliferation while it was cytotoxic for Caco-2 cells. Also, at 2.5 and 10 μM the complex stimulated type I collagen production. On the other hand, the behavior of the complex in relation to ALP activity follows the standard pattern for vanadium compounds, since the complex inhibited intestinal bovine ALP as well as the enzyme present in osteoblast cells. The cytotoxicity of the complex to both tumoral cell lines was also determined by analyzing the morphological alterations; apoptotic transformations of both cell lines were observed in a dose–response manner. In addition, the scavenging ability displayed by the complex might also contribute to the inhibition of the induction of tumoral processes by free radicals. The in vitro results indicate that the complex behaves as a more potent antitumoral agent for osteosarcoma than for colon adenocarcinoma. Overall, these results indicate that further evaluation of this complex as a candidate for antineoplastic treatments is required.

Acknowledgments The authors would like to gratefully acknowledge Dr. Luis Lezama (Departamento de Química Inorgánica, Facultad de Ciencia y Tecnología, Universidad del País Vasco, Apdo 644, 48080 Bilbao, Spain), who kindly measured the EPR spectrum. This work was supported by UNLP, CONICET (PIP6366), CICPBA, ANPCyT (PICT 10968). E.G.F. and S.B.E. are members of the Carrera del Investigador, CONICET. P.A.M.W is a member of the Carrera del Investigador CICPBA, Argentina. J.R. is a fellowship holder from CONICET and L.N. is a student fellow from CICPBA.

References

1. Hertog MG, Hollman PC, Katan MB, Kromhout D (1993) Nutr Cancer 20:21–29
2. Moridani MY, Pourahmad J, Bui H, Siraki A, O'brien PJ (2003) Free Radic Biol Med 34:243–253
3. Kostyuk VA, Potapovich AI, Vladykovskaya EN, Korkina LG, Afanas'ev IBA (2001) Arch Biochem Biophys 385:129–137
4. Bors W, Heller W, Michel C, Saran M (1990) Methods Enzymol 186:334–355
5. Peterson J, Dwyer M (1998) Nutr Res 18:1995–2018
6. Vinson JA, Dabbagh YA, Serry MM, Jang JH (1995) J Agric Food Chem 48:2800–2802
7. Kostyuk VA, Potapovich AI, Strigunova EN, Kostyuk TV, Afanas'ev IB (2004) Arch Biochem Biophys 428:204–208
8. Afanas'ev IB, Ostrakhovitch EA, Mikhal'chik EV, Ibragimova GA, Korkina LG (2001) Biochem Pharmacol 61:677–684
9. Middleton Jr E, Kandashwami C, Theoharides TC (2000) Pharmacol Rev 52:673–751
10. Ska-Kordala MS, Kowska AB, Ski J, Gabrielska JO (2001) Cell Mol Biol Lett 6:277–281
11. Ferrer EG, Salinas MV, Correa MJ, Naso L, Barrio DA, Etcheverry SB, Lezama L, Rojo T, Williams PAM (2006) J Biol Inorg Chem 11:791–801
12. Zhang J, Brodbelt JS, Wang J (2005) J Am Soc Mass Spectrom 16:139–151

13. Cos P, Ying L, Calomme M, Hu JP, Cimanga K, Poel BV, Pieters L, Vlietinck AJ, Berghe V (1998) J Nat Prod 61:71–76
14. Harborne JB, Williams CA (2000) Phytochemistry 55:481–504
15. Garg A, Garg S, Zaneveld LJ, Singla AK (2001) Phytother Res 15:655–669
16. Chiba H, Uehara M, Wu J, Wang X, Masuyama R, Suzuki K, Kanazawa K, Ishimi Y (2003) J Nutr 133:1892–1897
17. Miyagi Y, Om AS, Chee KM, Bennink MR (2000) Nutr Cancer 36:224–229
18. Kohno H, Taima M, Sumida T, Azuma Y, Ogawa H, Tanaka T (2001) Cancer Lett 174:141–150
19. Wilmsen PK, Spada DS, Salvador M (2005) J Agric Food Chem 53:4757–4761
20. Nielsen FH (1995) In: Segel H, Sigel A (eds) Metal ions in biological systems, vol 31. Dekker, New York, pp 543–573
21. Slebodnick C, Hamstra BJ, Pecoraro VL (1997) Struct Bonding 89:51–107
22. Crans DC, Smee JJ, Gaidamauskas E, Yang L (2004) Chem Rev 104:949–902
23. Williams PAM, Etcheverry SB (2007) Oxovanadium(IV) complexes with nonsteroidal antiinflammatory drugs (NSAIDs): pharmacological relevance. In: Aureliano Alves M (ed) Vanadium biochemistry. Research Signpost, India (in press)
24. Heyliger CE, Tahiliani AG, McNeil JH (1985) Science 227:1474–1477
25. Shechter Y (1990) Diabetes 39:1–5
26. Lampronti I, Bianchi N, Borgatti M, Fabbri E, Vizziello L, Hassan Khan MT, Ather A, Brezena D, Mahroof Tahir M, Gambari R (2005) Oncol Rep 14:9–15
27. Baran EJ (1997) Acta Farm Bonaerense 16:43–52
28. Morinville A, Maysinger D, Shaver A (1998) Trends Pharmacol Sci 19:452–460
29. Thompson KH, Orvig C (2001) Coord Chem Rev 219/221: 1033–1053
30. Rehder D (2003) Inorg Chem Commun 6:604–617
31. Baran EJ (2003) J Braz Chem Soc 14:878–888
32. Mukherjee B, Patra B, Mahaptra S, Banerjee P, Tiwari A, Chatterjee M (2004) Toxicol Lett 150:135–143
33. Beauchamp C, Fridovich I (1971) Anal Biochem 44:276–287
34. Iwamoto I, Mifuchi I (1982) Chem Pharm Bull 30:237–241
35. Kuo CC, Shih M, Kuo Y, Chiang W (2001) J Agric Food Chem 49:1654–1570
36. Yamaguchi T, Takamura H, Matoba TC, Terao J (1998) Biosci Biotechnol Biochem 62:1201–1204
37. Pellegrini RN, Proteggente A, Pannala A, Yang M, Rice-Evans C (1999) Free Radic Biol Med 26:1231–1237
38. Gorinstein S, Moncheva S, Katrich E, Toledo F, Arancibia P, Goshev I, Trakhtenberg S (2003) Mar Pollut Bull 46:1317–1325
39. Okajima T, Nakamura K, Zhang H, Ling N, Tanabe T, Yasuda T, Rozenfeld RG (1992) Endocrinology 130:2201–2212
40. Cortizo AM, Etcheverry SB (1995) Mol Cell Biochem 145: 97–192
41. Onishi M (1988) Photometric determination of traces of metals, part II, 4th edn. Wiley, New York
42. Etcheverry SB, Crans DC, Keramidas AD, Cortizo AM (1997) Arch Biochem Biophys 338:7–1462
43. Stein GS, Lian JB (1993) Endocr Rev 14:424–442
44. Bradford M (1976) Anal Biochem 72:248–254
45. Tullberg-Reinert H, Jundt G (1999) Histochem Cell Biol 112:271–276
46. Sálice VC, Cortizo AM, Gómez Dumm CL, Etcheverry SB (1999) Mol Cell Biochem 198:119–128
47. Tommasini S, Calabró ML, Stancanelli R, Donato P, Costa C, Catania S, Villari V, Ficarra P, Ficarra R (2005) J Pharm Biomed Anal 39:572–580
48. Horortz RR, Jurd L (1960) Acric Res Dev 26:2446–2447
49. Zhou J, Wang L, Wang J, Tang N (2001) J Inorg Biochem 83: 41–48
50. Hartley FR, Burgess C, Alcock RM (1980) Solution equilibria. Ellis Horwood, Chichester, UK, pp 44–45
51. Etcheverry SB, Williams PAM, Baran EJ (1997) Carbohydr Res 302:131–138
52. Williams PAM, Etcheverry SB, Baran EJ (2000) Carbohydr Res 329:41–47
53. Etcheverry SB, Barrio DA, Williams PAM, Baran EJ (2001) Biol Trace Elem Res 84:227–237
54. Yang L, Weng S, Ferraro JR, Wu J (2001) Vib Spectrosc 25: 57–62
55. Barrio DA, Williams PAM, Cortizo AM, Etcheverry SB (2003) J Biol Inorg Chem 8:459–468
56. Sreedhara A, Rao CP, Rao BJ (1996) Carbohydr Res 289:39–53
57. Weder JE, Dillon CT, Hambley TW, Kennedy BJ, Lay PA, Biffin JR, Regtop HL, Davies NM (2002) Coord Chem Rev 232:95–126
58. Gärtner A., Weser U (1986) Top Curr Chem 132:1–61
59. Roberts NA, Robinson PA (1985) Br J Rheumatol 24:128–136
60. Rajendran CM, Manisankar P, Gandhidasanm R, Murugesan R (2004) J Agric Food Chem 52:7389–7394
61. Barrio DA, Cattáneo ER, Apezteguía MC, Etcheverry SB (2006) Can J Physiol Pharmacol 84:765–775
62. Walter E, Kissel T (1995) Eur J Pharm Sci 3:215–230